

buffered by marble chips. At all  $\Sigma\text{SO}_4/\Sigma\text{Al(III)}$  ratios, we found substantial amounts of  $\text{Al(O)}_4$  and  $\text{Al(O)}_5$  in the flocs after separation from the marble chips.

A close genetic link between  $\text{Al}_{13}$  and solid aluminum hydroxides has been postulated (17, 18). However, the  $\text{Al}_{13}$  species is difficult to observe in nature because the pH window between formation and aggregation is small and because mixing of polluted and unpolluted waters is usually rapid and episodic. All of our results support the hypothesis that the aluminum flocs commonly found in polluted streams originate mainly from condensation of  $\text{Al}_{13}$  molecules that form rapidly and then aggregate as pH of the effluent increases to more than 5.

These results are important because  $\text{Al}_{13}$  is phytotoxic (5, 19) and is probably responsible for the decline of fish populations in rivers polluted by mine drainage and acid rain (20). Its longevity and chemical affinity for heavy-metal cations, such as  $\text{Pb}^{2+}$ ,  $\text{Cu}^{2+}$ , or  $\text{Zn}^{2+}$  (table S1) (21), suggest that dissolved  $\text{Al}_{13}$  and suspended aluminum flocs can transport metals downstream over considerable distances.

References and Notes

1. D. K. Nordstrom, *Geochim. Cosmochim. Acta* **46**, 681 (1982).
2. ———, J. W. Ball, *Science* **232**, 54 (1986).
3. K.-U. Ulrich, R. Pöthig, *Acta Hydrochim. Hydrobiol.* **28**, 313 (2000).
4. R. W. Smith, J. D. Hem, *U.S. Geol. Surv. Water Supply Pap.* **1827-D** (1972).
5. P. M. Bertsch, D. R. Parker, in *The Environmental Chemistry of Aluminum*, G. Sposito, Ed. (CRC Press, Boca Raton, FL, ed. 2, 1996), pp. 117–168.
6. Peak positions correspond to the data taken at 16.4 T, which are less affected by second-order quadrupolar shifts. Peak positions at 9.4 T are 3 to 5 ppm more negative than those at 16.4 T. Assignment of the peak near +35 ppm to  $\text{Al(O)}_5$  is based on the similarity of this chemical shift to those observed for crystalline phases that contain aluminum in coordination to five oxygens (22–25).
7. D. E. Woessner, *Am. Mineral.* **74**, 203 (1989).
8. A. Mason et al., *Environ. Sci. Technol.* **34**, 3242 (2000).
9. L. Allouche, C. Gérardin, T. Loiseau, G. Férey, F. Taulelle, *Angew. Chem. Int. Ed.* **39**, 511 (2000).
10. J. Rowsell, L. F. Nazar, *J. Am. Chem. Soc.* **122**, 3777 (2000).
11. D. K. Nordstrom, H. M. May, in *The Environmental Chemistry of Aluminum*, G. Sposito, Ed. (CRC Press, Boca Raton, FL, ed. 2, 1996), pp. 39–80.
12. G. Furrer, B. Trusch, C. Müller, *Geochim. Cosmochim. Acta* **56**, 3831 (1992).
13. G. Furrer, M. Gfeller, B. Wehrli, *Geochim. Cosmochim. Acta* **63**, 3069 (1999).
14. B. L. Phillips, W. H. Casey, M. Karlsson, *Nature* **404**, 379 (2000).
15. S. M. Bradley, R. A. Kydd, C. A. Fyfe, *Inorg. Chem.* **31**, 1181 (1992).
16. J.-P. Boisvert, C. Jolicœur, *Colloids Surf. A: Physicochem. Eng. Aspects* **155**, 161 (1999).
17. J. Y. Bottero et al., *J. Colloid Interface Sci.* **117**, 47 (1986).
18. D. Hunter, D. S. Ross, *Science* **251**, 1056 (1991).
19. D. R. Parker, T. B. Kinraide, L. W. Zelazny, *Soil Sci. Soc. Am. J.* **53**, 789 (1989).
20. A. B. S. Poleo, *Aquat. Toxicol.* **31**, 347 (1995).
21. B. Lothenbach, G. Furrer, R. Schulin, *Environ. Sci. Technol.* **31**, 1452 (1997).
22. M. C. Cruikshank et al., *J. Chem. Soc. Chem. Comm.* **1986**, 23 (1986).

23. L. B. Alemany, G. W. Kirker, *J. Am. Chem. Soc.* **108**, 6158 (1986).
24. B. L. Phillips, F. M. Allen, R. J. Kirkpatrick, *Am. Mineral.* **72**, 1190 (1987).
25. D. Massiott et al., *Magn. Reson. Chem.* **28**, S82 (1990).
26. G. Furrer, Chr. Ludwig, P. W. Schindler, *J. Colloid Interface Sci.* **149**, 56 (1992).
27. S. M. Bradley, R. A. Kydd, R. F. Howe, *J. Colloid Interface Sci.* **159**, 405 (1993).
28. The  $^{27}\text{Al}$  MAS NMR spectra were recorded in spring 2001 on a Chemagnetics CMX spectrometer at 104.25 MHz with single-pulse excitation, a pulse width of 1  $\mu\text{s}$ , a relaxation delay of 0.1 s, and a digitizing rate of 500 kHz. The samples were placed in sealed rotors (4-mm outside diameter) and spun at 15 to 16 kHz. The spinning sidebands lie outside of the displayed spectral range. Synthetic gel samples were examined wet, immediately after centrifugation, and after drying under ambient conditions, but no substantial difference was noted in the  $^{27}\text{Al}$  MAS NMR spectra. Additional spectra were taken several months later at 182.4 MHz with a Bruker Avance spectrometer and similar acquisition conditions, ex-

cept that the spinning rate was 30 kHz. These spectra are much better resolved and confirmed the estimates of relative populations of coordination environments.

29. The solutions were prepared by metathetic dissolution of the corresponding  $\text{Al}_{13}^-$  or  $\text{GaAl}_{12}$ -selenate crystals in the presence of dissolved  $\text{BaCl}_2$  (74, 15, 26, 27).
30. Financial support came from the NSF, the U.S. Department of Energy, and Eidgenössische Technische Hochschule Zürich. Much of the work was conducted at University of California, Davis, during G.F.'s sabbatical leave. We thank A. P. Lee, P. Yu, and M. Ziliox for technical assistance; B. Wehrli and A. C. Johnson for valuable discussions; and R. Schulin and L. Paul for general support. Inductively coupled plasma–mass spectrometry analyses were provided by A. Birkefeld.

Supporting Online Material

www.sciencemag.org/cgi/content/full/297/5590/2245/DC1  
 Figs. S2 to S4  
 Table S1

8 July 2002; accepted 16 August 2002

## Hydrogen Clusters in Clathrate Hydrate

Wendy L. Mao,<sup>1,2\*</sup> Ho-kwang Mao,<sup>2</sup> Alexander F. Goncharov,<sup>2</sup> Viktor V. Struzhkin,<sup>2</sup> Quanzhong Guo,<sup>2</sup> Jingzhu Hu,<sup>2</sup> Jinfu Shu,<sup>2</sup> Russell J. Hemley,<sup>2</sup> Maddury Somayazulu,<sup>3</sup> Yusheng Zhao<sup>4</sup>

High-pressure Raman, infrared, x-ray, and neutron studies show that  $\text{H}_2$  and  $\text{H}_2\text{O}$  mixtures crystallize into the sII clathrate structure with an approximate  $\text{H}_2/\text{H}_2\text{O}$  molar ratio of 1:2. The clathrate cages are multiply occupied, with a cluster of two  $\text{H}_2$  molecules in the small cage and four in the large cage. Substantial softening and splitting of hydrogen vibrons indicate increased intermolecular interactions. The quenched clathrate is stable up to 145 kelvin at ambient pressure. Retention of hydrogen at such high temperatures could help its condensation in planetary nebulae and may play a key role in the evolution of icy bodies.

Hydrogen-bonded  $\text{H}_2\text{O}$  frameworks form a remarkable number of pure ice phases (1–3) and can build polyhedron cages around guest molecules to form solid clathrate hydrates, thus trapping the guest molecules at temperatures and pressures at which they would otherwise exist as free gases (4–9). With each cage singly occupied by a guest molecule, clathrates at ambient pressure are limited to a guest/ $\text{H}_2\text{O}$  molecular ratio  $R \sim 1/6$  (Villard’s rule). Recently, multiple occupancy of the large cage in sII clathrate by small molecules has been recognized in high-pressure experiments (10–12) and theoretical simulations (13, 14). Dyadin et al. (12) suggested the possibility of  $R$  as high as 1/3. Hydrogen and water are by far the most

abundant gas and ice components in the solar system, but with a diameter of 2.72 Å, hydrogen molecules were thought to be too small to support a clathrate structure. Instead, hydrogen molecules were found to fill small cavities in ice II and ice Ic (15) at high pressures.

Here we report the synthesis of a hydrogen hydrate with the classical sII structure (HH-sII) with  $R = 0.45 \pm 0.05$  (16). This requires that the small cages be doubly occupied and the large cages be quadruply occupied by clusters of hydrogen molecules. HH-sII is stable (or metastable) to ambient pressure and low temperature after initial synthesis at a moderate pressure. In a diamond anvil cell (DAC), we compressed a mixture of  $\text{H}_2$  and  $\text{H}_2\text{O}$  to pressures of 180 to 220 MPa at 300 K. The samples were clearly separated into two regions: a  $\text{H}_2$  bubble and liquid water. Upon cooling to 249 K, the two fluids were observed to react and form a single, solid compound. These phases were monitored in situ using a variety of probes. Using energy-dispersive x-ray diffraction (EDXD) at the X17B beamline of the National Synchrotron Light Source (NSLS), we observed 21 diffraction peaks at  $220 \pm 30$  MPa and 234 K (table S1). The EDXD pattern in

<sup>1</sup>Department of the Geophysical Sciences, University of Chicago, Chicago, IL 60637, USA. <sup>2</sup>Geophysical Laboratory, Carnegie Institution of Washington, Washington, DC 20015, USA. <sup>3</sup>High Pressure Collaborative Access Team, Advanced Photon Source, Argonne National Laboratory, Argonne, IL 60439, USA. <sup>4</sup>Los Alamos Neutron Science Center (LANSCE), Los Alamos National Laboratory, Los Alamos, NM 87545, USA.

\*To whom correspondence should be addressed. E-mail: wmao@uchicago.edu

REPORTS

Fig. 1 can be indexed with a face-centered cubic unit cell with  $a = 17.047 \pm 0.010 \text{ \AA}$ , in excellent agreement with the archetypal sII clathrate (17). Time-of-flight neutron diffraction data collected at the High Intensity Powder Diffractometer instrument at LANSCE on a  $D_2$ - $D_2O$  sample in an aluminum cell confirmed the x-ray results of sII structure, but showed a slightly larger unit cell ( $a = 17.083 \pm 0.018 \text{ \AA}$  at 180 MPa and 220 K) due to the isotope effect and slightly different pressure and temperature ( $P$ - $T$ ) conditions. In the sII unit cell (Fig. 2), 136  $H_2O$  molecules form frameworks around eight hexakaidodecahedron ( $5^{12}6^4$ ) and 16 pentagonal dodecahedron ( $5^{12}$ ) cages (17). For  $R = 0.45 \pm 0.05$  (16), the 24 cages must be multiply occupied by  $H_2$  clusters to accommodate the  $61 \pm 7 H_2$  molecules (18). For close-packed clusters of two, three, four, five, and six  $H_2$ , the cluster diameters are 5.44, 5.86, 6.05, 6.57, and 6.57  $\text{\AA}$ , respectively, all smaller than the free cavity diameter of the  $5^{12}6^4$  cage (6.67  $\text{\AA}$ ) but larger than that of the  $5^{12}$  cage (5.02  $\text{\AA}$ ). However, the hydrogen molecules in the cluster are unbonded to one another, and the  $5^{12}$  cage could be considered as two separate cages each having a free cavity diameter of 3.27  $\text{\AA}$  that could easily accommodate a hydrogen molecule if the cluster axis is aligned toward opposite pentagonal faces (bimolecular cluster ordering) (Fig. 2). We attribute two  $H_2$  to each  $5^{12}$  cage and four  $H_2$  to each  $5^{12}6^4$  cage—that is, a total of 32  $H_2$  in  $5^{12}$  and 32  $H_2$  in  $5^{12}6^4$  per 136  $H_2O$  (19). In these cages, the intermolecular distances of  $H_2$  are not shortened but lengthened.

We used Raman spectroscopy to characterize bonding changes. At the formation of the clathrate, broad liquid water OH peaks at 3000 to 3600  $\text{cm}^{-1}$  transformed to sharp peaks typical of sII clathrates. Meanwhile, hydrogen roton peaks appeared at 300 to 850  $\text{cm}^{-1}$  and vibron peaks at 4100 to 4200  $\text{cm}^{-1}$  (Fig. 3). Hydrogen rotons,  $S_0(0)$ ,  $S_0(1)$ , and  $S_0(2)$ , in the clathrate were similar in frequency to those of pure hydrogen, indicating that the hydrogen molecules in clathrate cages were still in free rotational states. H-H vibrons of the new clathrate, on the other hand, are distinct from those of other known phases in the  $H_2$ - $H_2O$  system. In high-pressure  $H_2$ -filled ices, such as ice Ic (15), ice II (15), and ice Ih (20), the vibrons shift to higher frequencies relative to those of pure hydrogen; such a result indicates that the hydrogen molecules are squeezed in the small cavities and that the hydrates are only stable under confining pressures. In contrast, vibrons of HH-sII appear at 4120 to 4150  $\text{cm}^{-1}$  (Fig. 4), which is below the dominant  $Q_1(1)$  vibron at zero pressure (4155  $\text{cm}^{-1}$ ). This softening arises from increased intermolecular vibrational coupling within the  $H_2$  clusters and a substantial gas-to-crystal frequency shift (21). Attractive interactions between the hydrogen molecules and the host (even transfer of electron density) could

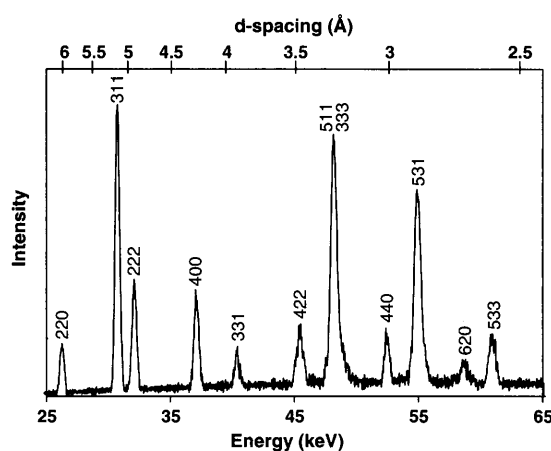


Fig. 1. EDXD pattern of  $H_2$ - $H_2O$  at 220 MPa and 234 K;  $2\theta = 4.50^\circ$ . The Miller indices  $hkl$  are marked on each peak. Because of the coarse crystallinity of the sample, peak intensities vary widely and cannot be used for structure refinement.

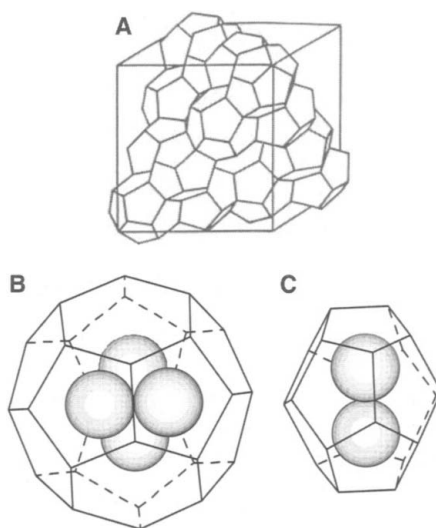


Fig. 2. (A) The sII crystal structure consisting of  $5^{12}6^4$  and  $5^{12}$  building blocks (17). (B) A tetrahedral cluster of four hydrogen molecules in the  $5^{12}6^4$  cage. (C) A cluster of two hydrogen molecules oriented toward opposite pentagonal faces in the  $5^{12}6^4$  cage. The  $H_2O$  frameworks define the edges of the polyhedrons, with an oxygen atom at each corner and a hydrogen atom on each edge. The  $5^{12}6^4$  and  $5^{12}$  cages are drawn to scale relative to the enclathrated hydrogen molecule (sphere) of 2.72  $\text{\AA}$  diameter.

result in additional stabilization of the clathrate without confining pressures. Once HH-sII was synthesized at 200 MPa, it showed remarkable stability (or metastability) and persisted to 280 K upon warming. Along another  $P$ - $T$  path, it was cooled to 78 K, and then pressure was released completely. The sample at 78 K was exposed to the vacuum ( $\sim 10 \text{ kPa}$ ) in the cryostat, and the clathrate remained.

Vibron spectra (Fig. 4) of the clathrate display two groups of multiplets of nearly equal intensities, supporting our assignment of two equal populations of hydrogen molecules in eight  $5^{12}6^4$  and 16  $5^{12}$  cages. We tentatively assign the lower frequency group at 4115 to 4135  $\text{cm}^{-1}$  to the loosely fitted tetrahedral molecular cluster in the  $5^{12}6^4$  cage and the higher

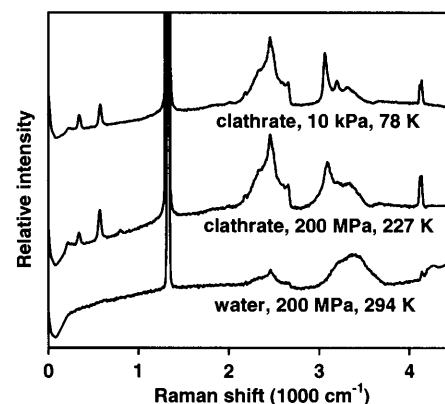


Fig. 3. Full-range Raman spectra showing the hydrogen molecular rotons  $S_0(0)$ ,  $S_0(1)$ , and  $S_0(2)$  at 355, 590, and 815  $\text{cm}^{-1}$ ; the first- and second-order peaks from the diamond anvil at 1336  $\text{cm}^{-1}$  and 2200 to 2600  $\text{cm}^{-1}$ , respectively; the OH peaks at 3000 to 3600  $\text{cm}^{-1}$ ; and the hydrogen molecular vibrons at 4100 to 4200  $\text{cm}^{-1}$ .

frequency group at 4135 to 4155  $\text{cm}^{-1}$  to the bimolecular cluster ordered in the  $5^{12}$  cage. Warming up from 78 K at 10 kPa, the higher frequency vibrons gradually vanished above 115 K while the lower frequency vibrons and the sII crystal structure persisted to 145 K. The observation is consistent with the above peak assignment, as the sII structure is known (6) to remain stable with filled  $5^{12}6^4$  cages and empty  $5^{12}$  cages (e.g.,  $SF_6 \cdot 17H_2O$ ). Above 145 K, the lower frequency vibrons gradually disappeared and the crystal structure collapsed. The multiple peaks within each group contain detailed information on the extent of intermolecular vibrational coupling, including configurational information (22).

Similar to the Raman vibron frequencies, infrared spectra of HH-sII also showed a hydrogen vibron peak at 4145  $\text{cm}^{-1}$  and a weak peak at 4120  $\text{cm}^{-1}$  (Fig. 5). Unlike the Raman vibron intensity, which is essentially intrinsic to the hydrogen molecule, the infrared vibron intensity is highly sensitive to the environment. Being a homonuclear molecule, the free hydrogen molecule does not have a permanent electric dipole moment and thus does not absorb infrared radiation. In a solid,

## REPORTS

**Fig. 4.** Raman spectra of the hydrogen clathrate in the hydrogen vibron region. The vertical dashed line marks  $Q_1(1) = 4155 \text{ cm}^{-1}$  for free hydrogen molecules at ambient conditions. The bottom spectrum shows 200-MPa  $Q_1(0)$ ,  $Q_1(1)$ ,  $Q_1(2)$ , and  $Q_1(3)$  peaks of fluid hydrogen at 4166, 4158, 4148, and  $4130 \text{ cm}^{-1}$ , shifted to higher energy relative to ambient condition peaks. The sequence of five spectra upward shows the  $P$ - $T$  evolution of HH-sII spectra: At 234 K and 200 MPa, vibrons consist of a low-frequency group at 4115 to  $4135 \text{ cm}^{-1}$  and a high-frequency group at 4135 to  $4155 \text{ cm}^{-1}$ ; cooling down to 99 K, each group shifts to slightly lower frequencies, sharpens, and displays clear triplets; decompressing to the low pressure of the cryostat ( $\sim 10 \text{ kPa}$ ), the vibrons do not change; warming to 144 K, the high-frequency group vanishes and the low-frequency group broadens and shifts to higher frequency; eventually the low-frequency peak diminishes at 150 K.

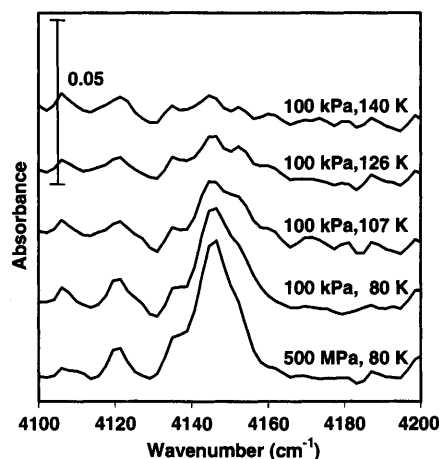
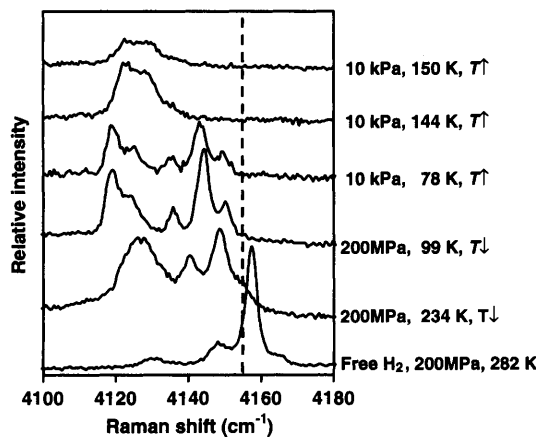


**Fig. 5.** Infrared spectra of the molecular hydrogen in clathrate. The vertical bar is an absorbance unit for a sample  $400 \mu\text{m}$  thick.

the hydrogen electron density can distort and exhibit collision-induced infrared absorption. The relatively strong  $4145 \text{ cm}^{-1}$  peak is coincident with the Raman mode assigned to the bimolecular cluster in the  $5^{12}$  cages; the  $4120 \text{ cm}^{-1}$  peak is also close to an observed Raman mode assigned to the tetrahedral cluster. Upon changing  $P$ - $T$  conditions, the infrared vibrons behave similarly to the Raman vibrons of the clathrate.

The first direct evidence (23) of molecular hydrogen frozen in interstellar ices was discovered in the IR spectrum of WL5, a deeply embedded protostar in the  $\rho$  Ophiuchus cloud complex. A weak absorption feature at  $4130$  to  $4150 \text{ cm}^{-1}$  in the WL5 spectrum was attributed to molecular hydrogen created by irradiation and frozen in situ into amorphous ices (23). The present infrared peaks of HH-sII (Fig. 5) match the WL5 spectra and provide an alternative explanation. Direct condensation of pure  $\text{H}_2$  requires temperatures  $< 3 \text{ K}$  (24), far below those of dense, molecular clouds (10 to 40

K). Practical models of hydrogen retention involve co-condensation with ices. For instance, experimental simulation reached a  $\text{H}_2/\text{H}_2\text{O}$  ratio up to 0.63 at 10 to 12 K (23, 25, 26). Most of the trapped hydrogen (80%) in the amorphous ice, however, escapes above 30 K. HH-sII provides a much more stable host for a large quantity of hydrogen to high temperatures. Because its synthesis pressure ( $> 180 \text{ MPa}$ ) is within the range of interior conditions of small, icy satellites, HH-sII could potentially hold hydrogen to high temperatures in bodies previously thought to be incapable of retaining hydrogen.

The kinetics of possible in situ formation HH-sII at low-pressure interstellar conditions has not yet been explored. However, considering the large hysteresis at low pressure, it is conceivable that this clathrate can be grown epitaxially on substrates of other sII clathrates or by annealing hydrogen in amorphous ices. Enclathration would also help to store hydrogen in larger bodies, from which it could be released gradually to form the hydrogen-rich atmosphere proposed for life-sustaining planets in interstellar space (27). The intriguing physics and chemistry of filling large cages with clusters of small molecules also opens new directions in clathrate and ice research. Finally, confining hydrogen molecular clusters in cages provides a new means for studying novel interactions and quantum effects, such as the proposed superfluidity and Bose-Einstein condensation of hydrogen molecular clusters [e.g., see (28–30)].

### References and Notes

- I.-M. Chou, J. G. Blank, A. F. Goncharov, H.-k. Mao, R. J. Hemley, *Science* **281**, 809 (1998).
- S. Klotz et al., *Nature* **398**, 681 (1999).
- V. F. Petrenko, R. W. Whitworth, *Physics of Ice* (Oxford Univ. Press, Oxford, 1999).
- H. Shimizu, T. Kumazaki, T. Kume, S. Sasaki, *J. Phys. Chem. B* **106** (2002).
- , *Phys. Rev. B* **65**, 212102 (2002).
- E. D. Sloan, *Clathrate Hydrates of Natural Gases* (Dekker, New York, ed. 2, 1997).

- J. S. Loveday et al., *Nature* **410**, 661 (2001).
- I.-M. Chou et al., *Proc. Nat. Acad. Sci. U.S.A.* **97**, 13484 (2000).
- H. Hirai et al., *J. Chem. Phys.* **115**, 7066 (2001).
- W. F. Kuhs, B. Chazallon, P. Radaelli, F. Pauer, J. Kipfstuhl, in *Proceedings of the 2nd International Conference on Natural Gas Hydrates* (Association PROGEP, Toulouse, France, 1999), pp. 9–16.
- Y. A. Dyadin et al., *Mendeleeev Commun.* **9**, 209 (1999).
- Y. A. Dyadin et al., *J. Struct. Chem.* **40**, 790 (1999).
- H. Itoh, J. S. Tse, K. Kawamura, *J. Chem. Phys.* **115**, 9414 (2001).
- E. P. VanKlaveren, J. P. J. Michels, J. A. Schouten, D. D. Klug, J. S. Tse, *J. Chem. Phys.* **114**, 5745 (2001).
- W. L. Vos, L. W. Finger, R. J. Hemley, H. K. Mao, *Phys. Rev. Lett.* **71**, 3150 (1993).
- The  $\text{H}_2/\text{H}_2\text{O}$  ratio ( $R$ ) of the compound was determined by three independent methods: (i) Direct microscopic observation through the diamond windows provided measurement of the volumes of the initial hydrogen bubble and  $\text{H}_2\text{O}$  liquid, the clathrate solid below 249 K, and the bubble and liquid after decomposition by warming to 280 K at 200 MPa. The measurement yielded  $R = 0.45$  with 10% uncertainty ( $\pm 0.05$ ), typical of gas-liquid volume determination in DAC by optical microscopy observation. (ii) The integrated intensities of hydrogen Raman vibrons are insensitive to the molecular environment and have been used previously for determination of  $R$  in hydrogen-filled ices (75). The amount of  $\text{H}_2$  per unit volume of HH-sII was estimated from the vibron intensity ratio of the HH-sII region to the hydrogen bubble region (density from the known equation of state of fluid hydrogen) of the same thickness at the same  $P$ - $T$  condition, and the amount of  $\text{H}_2\text{O}$  per unit volume of HH-sII was obtained from x-ray and neutron unit cell determination. The Raman intensity ratio yielded  $R = 0.48 \pm 0.04$  for HH-sII. (iii) The volume ratio of the empty space (to be filled by  $\text{D}_2$ ) to the injected liquid  $\text{D}_2\text{O}$  in the  $600\text{-mm}^3$  sample chamber of the aluminum cell set an upper limit of  $R < 0.5$ .
- T. C. W. Mak, R. K. McMullan, *J. Chem. Phys.* **42**, 2732 (1965).
- The polycrystalline x-ray and neutron diffraction data were excellent for determination of unit cell parameters but were insufficient for refinement of multiple cage occupancy and orientation ordering in the cages. Ideally, single-crystal neutron diffraction data are needed for such refinement.
- Other combinations of multiple occupancy, such as one  $\text{H}_2$  molecule in each  $5^{12}$  cage and six  $\text{H}_2$  molecules in each  $5^{12}6^4$  cage, can also accommodate the total of 64  $\text{H}_2$  molecules but are inconsistent with the Raman observations.
- H. L. Strauss, Z. Chen, C.-K. Loong, *J. Chem. Phys.* **101**, 7177 (1994).
- H. K. Mao, R. J. Hemley, *Rev. Mod. Phys.* **66**, 671 (1994).
- W. L. Mao, H.-k. Mao, A. F. Goncharov, V. V. Struzhkin, R. J. Hemley, in preparation.
- S. A. Sandford, L. J. Allamandola, T. R. Geballe, *Science* **262**, 400 (1993).
- T. J. Lee, *Nature* **237**, 99 (1972).
- Y. A. Dyadin, E. Y. Aladko, K. A. Udachin, M. Tkacz, *Pol. J. Chem.* **68**, 343 (1994).
- D. Laufer, E. Kochavi, A. Bar-Nun, *Phys. Rev. B* **36**, 9219 (1987).
- D. J. Stevenson, *Nature* **400**, 32 (1999).
- V. Ginzburg, A. Sobyanyin, *JETP Lett.* **15**, 242 (1972).
- T. E. Huber, C. A. Huber, *Phys. Rev. Lett.* **59**, 1120 (1987).
- E. L. Knuth, F. Schünemann, J. P. Toennies, *J. Chem. Phys.* **102**, 6258 (1995).
- We thank NSLS and LANSCE for synchrotron and neutron beam time and technical support, and S. Stishov for use of the aluminum pressure cell. Supported by the NSF Earth Science Division, the NASA Planetary Geology and Geophysics Program, the U.S. Department of Energy (Basic Energy Research), the W. M. Keck Foundation, and the Carnegie Institution of Canada.

### Supporting Online Material

www.sciencemag.org/cgi/content/full/297/5590/2247/DC1 Table S1

24 June 2002; accepted 29 August 2002